

Dark energy and key physical parameters of clusters of galaxies

G.S. Bisnovaty-Kogan¹ • A.D. Chernin²

Abstract We study physics of clusters of galaxies embedded in the cosmic dark energy background. Under the assumption that dark energy is described by the cosmological constant, we show that the dynamical effects of dark energy are strong in clusters like the Virgo cluster. Specifically, the key physical parameters of the dark matter halos in clusters are determined by dark energy: 1) the halo cut-off radius is practically, if not exactly, equal to the zero-gravity radius at which the dark matter gravity is balanced by the dark energy antigravity; 2) the halo averaged density is equal to two densities of dark energy; 3) the halo edge (cut-off) density is the dark energy density with a numerical factor of the unity order slightly depending on the halo profile. The cluster gravitational potential well in which the particles of the dark halo (as well as galaxies and intracluster plasma) move is strongly affected by dark energy: the maximum of the potential is located at the zero-gravity radius of the cluster.

Keywords dark energy; galaxy cluster

1 Introduction

It has recently been recognized that galaxies and clusters of galaxies (as well as all the other bodies of nature) are imbedded in the universal dark energy background discovered first by Riess et al. (1998) and Perlmutter et al. (1999) in observations of SNe type Ia at the global horizon-size distances ~ 1000 Mpc. These

and other observations and in particular the studies of the cosmic microwave background (CMB) anisotropy Spergel et al. (2007) indicate that the global dark energy density $\rho_\Lambda = 0.7 \times 10^{-29}$ g/cm³, and dark energy contributes nearly 3/4 to the total energy content of the universe. Close value of the cosmological constant was anticipated by Kofman and Starobinskii (1985), basing on the analysis of the existing upper limits for the microwave background anisotropy. According to the simplest, straightforward and quite likely interpretation adopted in the standard Λ CDM cosmology, dark energy is represented by the Einstein cosmological constant Λ and its density $\rho_\Lambda = \frac{c^2}{8\pi G}\Lambda$, where G is the gravitational constant. If this is so, dark energy is the energy of the cosmic vacuum Gliner (1966) and it may be described macroscopically as a perfectly uniform fluid with the equation of state $p_\Lambda = -\rho_\Lambda$ (here p_Λ is the dark energy pressure; the speed of light $c = 1$ hereafter). It is this standard interpretation that implies that although dark energy betrayed its existence through its effect on the universe as a whole, it exists everywhere in space with the same density and pressure.

Dark energy treated as Λ -vacuum produces anti-gravity, and at the present cosmic epoch, the anti-gravity is stronger than the gravity of matter for the global universe considered as a whole. May the dynamical effects of dark energy be strong on smaller scales as well? Local dynamical effects of dark energy were first recognized by Chernin et al. (2003); the studies of the Local Group of galaxies and the expansion outflow of dwarf galaxies around it revealed that the antigravity may dominate over the gravity at distance of $\simeq 1 - 3$ Mpc from the barycenter of the group (Chernin 2001, 2008; Baryshev et al. 2001; Karachentsev et al. 2009; Byrd et al.; Teerikorpi et al. 2008; Teerikorpi and Chernin 2010). It was also demonstrated that this is the smallest astronomical scale on

G.S. Bisnovaty-Kogan

Space Research Institute, Russian Academy of Sciences, Moscow, Russia

A.D. Chernin

Sternberg Astronomical Institute, Moscow University, Moscow, Russia

which the antigravity produced by the dark energy background may be stronger than the matter gravity.

Further studies Chernin et al. (2010) show that the nearest rich cluster of galaxies, the Virgo cluster and the Virgocentric expansion outflow around form a system which is a scale-up version of the Local Group with its expanding environment. It proves that the matter gravity dominates in the volume of the cluster, while the dark energy antigravity is stronger than the matter gravity in the Virgocentric outflow at the distances of $\simeq 10 - 30$ Mpc from the cluster center. On both scales of 1 and 10 Mpc, the key physical parameter of the system is its "zero-gravity radius" which is the distance (from the system center) where the matter gravity and the dark energy antigravity balance each other exactly. The gravitationally bound system can exist only within the sphere of this radius; outside the sphere the flow dynamics is controlled mostly by the dark energy antigravity.

Abdalla et al. (2009) used optical, X-ray and weak lensing data on 33 relaxed galaxy clusters to study the dark energy signature in the virial structure of clusters. A new treatment has been provided for spherically collapsing system where dark energy does not cluster together with dark matter (He et al. 2010). The spherical collapse in quintessence models with zero speed of sound was studied (Creminelli et al. 2010). Perturbations in DE, which is not identical with a cosmological constant, had been investigated by (Creminelli and Senatore 2007),(Creminelli et al. 2009). The static solutions for polytropic configurations, and their dynamic stability, in presence of the cosmological constant, have been investigated numerically by Merafina et al. (2012).

In this paper, we focus mostly on the cluster interior. Having in mind the Virgo cluster as an archetypical example, we consider a cluster as a gravitationally bound quasi-spherical configuration of cold non-relativistic collisionless dark matter and baryonic matter in the cosmological proportion. In addition, omnipresent dark energy with the cosmological density ρ_Λ is contained in the same volume. In Sec.2, we give a brief account of the theory relations that describe the antigravity force field produced by dark energy in terms of the Newtonian mechanics and show that the zero-gravity radius may serve as a natural cut-off radius for the dark matter halo of a cluster. This suggests some basic interconnections that involves the matter mass, the size and the galaxy velocity dispersion of the cluster (Sec.3). In Secs.4,5 we address physical parameters of dark halos in cluster halo and clarify how the presence of the dark energy background restricts their values as well as the deepness of the gravitational potential well

of the cluster. A brief discussion of the results is given in Sec.6.

1.1 Dark energy on the cluster scale

Dark energy is a relativistic fluid and its description is based on General Relativity. Nevertheless it may be treated in terms of the Newtonian mechanics, if the force field it produces is weak in the ordinary accepted sense. The Newtonian treatment borrows from General Relativity the major result: the effective gravitating density of a uniform medium is given by the sum

$$\rho_{eff} = \rho + 3p. \quad (1)$$

With its equation of state $p_\Lambda = -\rho_\Lambda$, dark energy has the negative effective gravitating density:

$$\rho_{\Lambda eff} = \rho_\Lambda + 3p_\Lambda = -2\rho_\Lambda < 0. \quad (2)$$

It is because of this negative value that dark energy produces antigravity.

With this result, one may introduce "Einstein's law of universal antigravity" which says that two bodies imbedded in the dark energy background undergo repulsion from each other with the force which is proportional to the distance r between them:

$$F_E(r) = -\frac{4\pi G}{3}\rho_{\Lambda eff}r^3/r^2 = +\frac{8\pi G}{3}\rho_\Lambda r. \quad (3)$$

(This is the force for the unit mass of the body.) Let us consider a spherical mass M of non-relativistic matter embedded in the dark energy background. A test particle at the distance r from the mass center (and out of the mass) has the radial acceleration in the reference frame related to the mass center:

$$F(r) = F_N(r) + F_E(r) = -G\frac{M}{r^2} + \frac{8\pi G}{3}\rho_\Lambda r. \quad (4)$$

Note that (4) comes directly from the Schwarzschild-de Sitter spacetime in the weak field approximation, see, for instance, Chernin et al. (2006); (4) may also be used for the mass interior; in this case $M = M(r)$ in (4), see Merafina et al. (2012).

It is seen from (4) that the total force F and the acceleration are both zero at the distance

$$r = R_\Lambda = \left[\frac{M}{\frac{8\pi}{3}\rho_\Lambda}\right]^{1/3}. \quad (5)$$

Here R_Λ is the zero-gravity radius (Chernin et al. 2003; Chernin 2001, 2008). The gravity dominates at distances $r < R_\Lambda$, the antigravity is stronger than the gravity at $r > R_\Lambda$. It implies that the gravitationally bound system with the mass M can exist only within

the zero-gravity sphere of the radius R_Λ . Clusters of galaxies are known as the largest gravitationally bound systems. Thus, the zero-gravity radius is an absolute upper limit for the radial size R of a static cluster:

$$R < R_\Lambda = \left[\frac{M}{\frac{8\pi}{3}\rho_\Lambda} \right]^{1/3}. \quad (6)$$

The total mass of the Virgo cluster estimated by Karachentsev and Nasonova (2010) with the "zero-velocity" method is $M = (6.3 \pm 2.0) \times 10^{14} M_\odot$. This result agrees well with the earlier virial mass of the cluster $M_{vir} = 6 \times 10^{14} M_\odot$ estimated by Hoffman and Salpeter (1982). (Teerikorpi et al. 1992; Ekholm et al. 1999, 2000) found that the real cluster mass M might be from 1 to 2 the virial mass: $M = (0.6 - 1.2) \times 10^{15} M_\odot$. Tully and Mohayaee (2004) obtained the Virgo cluster mass $M = 1.2 \times 10^{15} M_\odot$. Taking for an estimate the total mass of the Virgo cluster (dark matter and baryons) $M = (0.6 - 1.2) \times 10^{15} M_\odot$ and the cosmological dark energy density ρ_Λ (see Sec.1), one finds the zero-gravity radius of the Virgo cluster:

$$R_\Lambda = (9 - 11) Mpc \simeq 10 \text{ Mpc}. \quad (7)$$

For the richest clusters like the Coma cluster with the masses $\simeq 10^{16} M_\odot$ the zero-gravity radius may have the values about 20 Mpc. Recent most systematic data on velocities and distances of galaxies in the Virgo cluster and the Virgocentric flow around it are presented in the Hubble diagram for the distances up to 30 Mpc from the cluster center Karachentsev and Nasonova (2010). The diagram reproduced (with some modifications) in Fig.1 reveals clearly a two-component structure in the velocity-distance ($v - r$) phase space: there is the inner area which is the cluster itself and the outer area of the Virgocentric flow. We countered the areas roughly with bold dashed lines in Fig.1. The positive and negative velocities are seen in the cluster in practically equal numbers, so the inner component is quite symmetrical relative to the horizontal line $v = 0$. The velocities range is -2 000 to +1700 km/s there, and the mean velocity dispersion $V \simeq 700$ km/s. The "border" zone between the components is in the distance range $6 < R < 12$ Mpc; it is poorly populated in the diagram, and the velocities are considerably less scattered: they are from -400 to + 600 km/s, in the zone. The Virgocentric flow with only positive velocities is seen at distances > 12 Mpc; the flow area is roughly symmetrical relative to a beam from the coordinate origin $V = H_{Virgo} R$, with the local (Virgo) Hubble factor $H_{Virgo} = 58$ km/s/Mpc.

We see that the zero-gravity radius calculated for the Virgo cluster (5,7) is certainly within the border

zone between the two areas of the Hubble diagram: $6 < R_\Lambda < 12$ Mpc. This fact suggests that the zero-gravity radius calculated for the Virgo cluster coincides approximately, if not exactly, with the radius of the inner component of the system in Fig.1.

2 Cluster overall parameters

The data of the Hubble diagram for the Virgo system (see Fig.1) enable us to obtain another approximate empirical equality:

$$\left[\frac{RV^2}{GM} \right]_{Virgo} \simeq 1. \quad (8)$$

This dimensionless combination of the overall physical parameters of the cluster resembles the traditional virial relation. However its physical sense is different from that of the virial theorem, which has a form for the polytropic star with the polytropic index n

$$\varepsilon_g = -\frac{n}{3}\varepsilon_g + \frac{2n}{3}\varepsilon_\Lambda,$$

see Merafina et al. (2012).

The equation (8) does not assume any kind of equilibrium state of the system; it does not assume either any special relation between the kinetic and potential energies of the system. It assumes only that the system is embedded in the dark energy background and it is gravitationally bound.

The data on the Local Group ((Karachentsev et al. 2009; Chernin et al. 2009)) show in combination with (8) that

$$\left[\frac{RV^2}{GM} \right]_{Virgo} \simeq \left[\frac{RV^2}{GM} \right]_{LG} \simeq 1. \quad (9)$$

Here we use for the Local Group the following empirical data: $R \simeq 1$ Mpc, $M \simeq 10^{12} M_\odot$, $V \simeq 70$ km/s which give the radius, the total mass and the velocity dispersion in the Local Group, correspondingly (Karachentsev et al. (2009)).

Equation (9) indicates that there is a similarity (in the sense of the similarity theory) between the gravitationally bound systems of 1 Mpc scale and 10 Mpc scale. This seemingly provides us with an evidence that such a similarity exists not only for the Virgo System and the Local System, but for any systems of the group and cluster scale – at least roughly.

Assuming that the bound inner component (the cluster) of the Virgo system has a zero-gravity radius R_Λ (6), we obtain from the empirical relation (9) that

$$V^2 \simeq \left(\frac{8\pi}{3} \right)^{1/3} GM^{2/3} \rho_\Lambda^{1/3}. \quad (10)$$

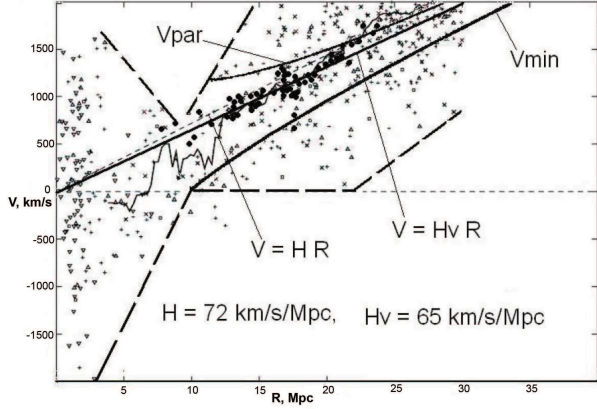


Fig. 1 The Hubble diagram for 761 galaxies of the Virgo Cluster and Virgocentric flow with Virgocentric velocities and distances Karachentsev and Nasonova (2010). A two-component phase structure (countered by the bold dashed lines) is clearly seen in the diagram: the central component is the bound quasi-stationary cluster and the other one is the Virgocentric flow. The matter gravity dominates the cluster, the dark energy antigravity is stronger than gravity in the flow. The zero-gravity radius $R_\Lambda = 9 - 11$ Mpc is located in the less populated zone between the components. The broken line is the running median which used by Karachentsev and Nasonova (2010) to find the zero-velocity radius $R_0 = 6 - 7$ Mpc. Two beams from the coordinate center are the lines $V \propto R$ with the Hubble factors $H = 72$ km/s/Mpc (the dashed one) and $H_V = 65$ km/s/Mpc. The galaxies with the most accurate distances and velocities are marked by filled circles in the area of the Virgocentric flow. The galaxies of this subsample follow well the line with H_V which is the median beam for them. The curve V_{par} is the flow trajectory with zero total mechanical energy; the curve V_{min} is the trajectory with the minimal escape velocity from the potential well of the cluster. The most accurate data occupy the area between the two curves.

As we see, the velocity dispersion in the gravitationally bound system depends only on its mass and the universal dark energy density. The relation (10) enables one to estimate the matter mass of a cluster, if its velocity dispersion is measured in observations:

$$M \simeq G^{-3/2} \left[\frac{8\pi}{3} \rho_\Lambda \right]^{-1/2} V^3 \simeq 10^{15} \left[\frac{V}{700 \text{ km/s}} \right]^3 M_\odot. \quad (11)$$

From the other side, the approximate empirical relation (9) may serve as an estimator of the local dark energy density, ρ_{loc} . Indeed, if the mass of a cluster and its velocity dispersion are independently measured, one has:

$$\rho_{loc} \simeq \frac{3}{8\pi G^3} M^{-2} V^6 \simeq \rho_\Lambda \left[\frac{M}{10^{15} M_\odot} \right]^{-2} \left[\frac{V}{700 \text{ km/s}} \right]^6, \quad (12)$$

what indicates that the observational data on the Local System and the Virgo System provide strong evidence in favor of the universal value of the dark energy density which is the same on both global and local scales.

3 Dark matter halos

The similarity between the Virgo cluster and the Local Group in terms of their overall parameters (9) does not extend to the internal structure of the systems. As is well-known, the mass of the Local Group is mainly contained in the two dark matter halos of the M31 Galaxy and the Milky Way. In this sense, internal dynamics of the group is reduced – in the first approximation – to the two-body problem describing the relative motion of the two giant galaxies (see, for instance, Chernin et al. (2009)). Contrary to that, galaxies of the Virgo cluster move in a common dark matter halo of the cluster as a whole, and the dark matter of the halo is smoothly distributed over the cluster volume. Observations and computer simulations indicate – in acceptable agreement with each other – that the spherically-averaged density profiles of the halos in various clusters are rather regular and reveal a simple dependence on the radial distance.

In the simplest case, the halo density profile may be approximated by the isothermal power law:

$$\rho = \rho_1 \left(\frac{r_1}{r} \right)^2, \quad (13)$$

where ρ_1, r_1 are two constants; $\rho_1 = \rho(r_1)$. It was demonstrated (for $\Lambda = 0$) that the density profile of (13) may exist in a system of particles moving along circular orbits (Bisnovatyi-Kogan and Zel'Dovich

(1969)) and in systems with almost radial orbits as well (Antonov and Chernin (1975)).

According to the considerations of the section above, the zero-gravity radius of a cluster like the Virgo cluster is roughly (or maybe exactly) equal to the total radius of the halo. If this is the case, we may identify r_1 with $R = R_\Lambda$, and ρ_1 is then the dark matter density at the halo's outer edge ρ_{edge} . With this, we find the total mass of the halo:

$$M = 4\pi \int_0^R \rho r^2 dr = 4\pi \rho_{edge} R_\Lambda^3. \quad (14)$$

On the other hand, $M = \frac{8\pi}{3} \rho_\Lambda R_\Lambda^3$; then (14) gives:

$$\rho_{edge} = \frac{2}{3} \rho_\Lambda. \quad (15)$$

The cut-off density $\rho_1 = \rho(R_\Lambda)$ proves to be a constant value which does not depend on the total mass or velocity dispersion of the isothermal halo; the density is just the universal dark energy density with the order-of-unity numerical factor.

It follows from (14) that the mean halo density, $\langle \rho \rangle$, is given again by the dark energy density, but with another numerical factor:

$$\langle \rho \rangle = 3\rho_{edge} = 2\rho_\Lambda. \quad (16)$$

The last relation is obviously valid for any halo's profile, not only for the isothermal one.

Another example is a halo with the "pseudo-isothermal" profile:

$$\rho(r) = \frac{\rho_c}{1 + (\frac{r}{r_c})^2}, \quad (17)$$

where ρ_c is the central core density, $\rho_c = \rho(r_c)$; and r_c is the core radius. The total mass of the halo

$$M = 4\pi \rho_c r_c^3 \left(\frac{R}{r_c} - \arctan \frac{R}{r_c} \right). \quad (18)$$

On the other hand, we have for the total mass a relation $M = \frac{8\pi}{3} \rho_\Lambda R_\Lambda^3$. Then (18) gives:

$$\rho_c = \frac{2}{3} \rho_\Lambda \frac{\alpha^3}{\alpha - \arctan \alpha}, \quad (19)$$

where $\alpha = \frac{R_\Lambda}{r_c}$. Here the cut-off density

$$\rho_{edge} = \frac{\rho_c}{1 + \alpha^2} = \frac{2}{3} \frac{\rho_\Lambda \alpha^3}{(\alpha - \arctan \alpha)(1 + \alpha^2)}. \quad (20)$$

If the core radius is much smaller than the zero-gravity radius, $\alpha \gg 1$, (20) gives the same result as (16). If, for instance, $\alpha = 3$, then $\rho_c \simeq 10\rho_\Lambda$ and $\rho(R_\Lambda) \simeq \rho_\Lambda$. If $\alpha = 10$, then $\rho_c \simeq 80\rho_\Lambda$ and $\rho(R_\Lambda) \simeq 0.8\rho_\Lambda$.

One of possible halo profiles is suggested by computer simulations of a large-scale structure formation – this is the "universal" profile introduced by Navarro et al. (1996):

$$\rho(r) = \frac{4\rho_s}{\frac{r}{r_s} \left(1 + \frac{r}{r_s} \right)^2}, \quad (21)$$

where $\rho_s = \rho(r_s)$. The total halo mass

$$M = 16\pi \rho_s r_s^3 \left[\ln(1 + \beta) - \frac{\beta}{1 + \beta} \right], \quad (22)$$

where $\beta = \frac{R}{r_s}$. The two characteristic densities:

$$\rho_s = \frac{1}{6} \frac{\rho_\Lambda \beta^3}{\ln(1 + \beta) - \frac{\beta}{1 + \beta}}, \quad (23)$$

$$\rho_{edge} = \frac{2}{3} \frac{\rho_\Lambda \beta^2}{\left[\ln(1 + \beta) - \frac{\beta}{1 + \beta} \right] (1 + \beta)^2}. \quad (24)$$

If $\beta \gg 1$,

$$\rho_s \simeq \frac{1}{6} \frac{\rho_\Lambda \beta^3}{\ln \beta - 1}, \quad (25)$$

$$\rho_{edge} = \frac{2}{3} \frac{\rho_\Lambda}{\ln \beta - 1}. \quad (26)$$

If $\beta = 3$, we have $\rho_s \simeq 8\rho_\Lambda$ and $\rho_{edge} \simeq 0.5\rho_\Lambda$. If $\beta = 10$, then $\rho_s \simeq 20\rho_\Lambda$ and $\rho_{edge} \simeq 0.2\rho_\Lambda$.

Finally, the Einasto profile (Einasto and Haud (1989)) seems to be currently most popular:

$$\rho(r) = \rho_c \exp\left[-\left(\frac{r}{r_e}\right)^n\right], \quad (27)$$

where $\rho_c = \rho(0)$, and the constant exponent n lies in between 0.1 and 0.3. Putting $r_e = \frac{1}{N} R_\Lambda$, where $N \geq 1$ is a constant, and suggesting $r_{edge} = R_\Lambda$ we find the central density:

$$\rho_c = \frac{2}{3} \frac{N^3}{I(n, N)} \rho_\Lambda, \quad (28)$$

where

$$I(n, N) = \int_0^N x^2 \exp[-x^n] dx. \quad (29)$$

Then the edge density

$$\rho_{edge} = \rho_c \exp[-N^n]. \quad (30)$$

The numbers $s = \frac{\rho_c}{\rho_\Lambda}$ and $q = \frac{\rho_{edge}}{\rho_\Lambda}$ are given in Tables 1,2 for $n = 0.1; 0.2; 0.3$ and $N = 1; 3; 10$.

As we see, the antigravity produced by dark energy puts a clear limit to the extension of dark matter halos

in clusters: the halo may exist only in the area $r \leq R_\Lambda$ where the antigravity is weaker than the gravity produced by non-vacuum matter of the cluster. The dark energy density determines the mean matter density of the halo and its edge (cut-off) density. These are the three key physical parameters of clusters.

3.1 Cluster potential well

Clusters of galaxies are the largest gravitationally bound systems in the universe. Each cluster is located in its gravitational potential well which is the volume where galaxies, gas particles and particles of the dark matter move along finite orbits. We will show now that the structure of the potential well is strongly affected by the dark energy background in which clusters are embedded.

The gravitational potential $\Phi(r)$ inside the cluster comes from the Poisson equation:

$$\Delta\Phi = 4\pi G(\rho - 2\rho_\Lambda). \quad (31)$$

Restricting ourselves for simplicity by the model of the isothermal halo, we find from (31) together with (14),(16):

$$\frac{d\Phi}{dr} = -\frac{8\pi G}{3}\rho_\Lambda r \left[1 - \left(\frac{R_\Lambda}{r}\right)^2\right], \quad 0 \leq r \leq R_\Lambda. \quad (32)$$

In accordance with what was said above, the acceleration $-\frac{d\Phi}{dr} = 0$ at $r = R_\Lambda$. The extremum (maximum) of the potential Φ is located at the same distance $r = R_\Lambda$.

The potential comes from integration of (32):

$$\Phi(r) = -\frac{4\pi G}{3}\rho_\Lambda r^2 \left[1 - 2\left(\frac{R_\Lambda}{r}\right)^2 \ln \frac{r}{R_\Lambda}\right] + C. \quad (33)$$

The constant C may be found from the boundary condition at $r = R_\Lambda$:

$$\Phi(R_\Lambda) = -\frac{4\pi G}{3}\rho_\Lambda R_{ZG}^2 + C = -\frac{4\pi G}{3}\rho_\Lambda R_\Lambda^2 - \frac{GM}{R_\Lambda}. \quad (34)$$

Table 1 The ratio $s = \frac{\rho_c}{\rho_\Lambda}$ from (28), for different parameters n and N

N	n	0.1	0.2	0.3
1		5.261	5.097	4.946
3		5.886	6.413	7.029
10		6.758	8.797	12.09

It implies that $C = -\frac{GM}{R_\Lambda}$. Then the maximum of the potential

$$\Phi_{max} = -\frac{3}{2}\frac{GM}{R_\Lambda} = -\frac{3}{2}G\left(\frac{8\pi}{3}\rho_\Lambda\right)^{1/3}M^{2/3}. \quad (35)$$

The value of Φ_{max} depends on the cluster matter mass M and the universal dark energy density. Its value is the same for any halo profile. It gives a quantitative measure to the deepness of the cluster potential well and determines the characteristic isothermal velocity of the gravitationally bound particles (galaxies, intra-cluster plasma particles and dark matter particles) in the cluster:

$$\begin{aligned} V_{iso} &= |\Phi_{max}|^{1/2} = G^{1/2}\left(\frac{3}{2}\right)^{1/2}\left(\frac{8\pi}{3}\rho_\Lambda\right)^{1/6}M^{1/3} \\ &= 780\left[\frac{M}{10^{15}M_\odot}\right]^{1/3}. \end{aligned} \quad (36)$$

As we see, this velocity is rather close to the mean velocity dispersion, $V \simeq 700$ km/s, of the galaxies in the Virgo cluster (Sec.3); $V_{iso} \simeq V$ also for the Coma cluster with its matter mass $M \simeq 10^{16}M_\odot$ and $V \simeq 1000$ km/s.

The plasma isothermal temperature

$$\begin{aligned} T_{iso} &= \frac{Gm}{3k}V_{iso}^2 = \frac{m}{3k}\left(\frac{8\pi}{3}\rho_\Lambda\right)^{1/3}M^{2/3} \\ &= 3 \times 10^7 \left[\frac{M}{10^{15}M_\odot}\right]^{2/3}K, \end{aligned} \quad (37)$$

where k, m are the Boltzmann constant and the hydrogen atom mass. The temperature of (37) is roughly equal to the temperature of the hot X-ray emitting plasma in clusters like the Virgo cluster or the Coma cluster.

Identifying theoretical value V_{iso} with the observed value V for typical clusters, we see that the matter mass of a cluster can be estimated, if the velocity dispersion

Table 2 The ratio $q = \frac{\rho_{edge}}{\rho_\Lambda}$ from (30), for different parameters n and N

N	n	0.1	0.2	0.3
1		1.9354	1.875	1.820
3		1.928	1.845	1.750
10		1.919	1.803	1.644

of its galaxies is measured:

$$M = \left(\frac{2}{3G}\right)^{3/2} \left(\frac{8\pi}{3}\rho_\Lambda\right)^{-1/2} V_{iso}^3 = 10^{15} M_\odot \left(\frac{V}{780 \text{ km/s}}\right)^3. \quad (38)$$

The relation $M \propto V^3$ agrees well with the empirical relation (11). In a similar way, the mass may be found, if the theoretical value of the temperature T_{iso} is identified with the measured temperature of the intracluster plasma:

$$M = \left(\frac{3k}{Gm}\right)^{3/2} \left(\frac{8\pi}{3}\rho_\Lambda\right)^{-1/2} T_{iso}^{3/2} \quad (39)$$

$$= \left(\frac{T}{2 \times 10^7 \text{ K}}\right)^{3/2} \times 10^{15} M_\odot.$$

Finally, if the matter mass of a cluster and its velocity dispersion or its plasma temperature are measured independently, (36)-(39) enable one to estimate the local density of dark energy:

$$\rho_{loc} = \rho_\Lambda \left(\frac{M}{10^{15} M_\odot}\right)^{-2} \left(\frac{V}{780 \text{ km/s}}\right)^6, \quad (40)$$

$$\rho_{loc} = \rho_\Lambda \left(\frac{M}{10^{15} M_\odot}\right)^{-2} \left(\frac{T}{3 \times 10^7 \text{ K}}\right)^3. \quad (41)$$

It is seen from (35),(36), the empirical data on clusters like the Virgo cluster or the Coma cluster are completely consistent with our starting assumption that the local density of dark energy on the scale of clusters of galaxies is the same as on the global cosmological scales.

4 Conclusions

Dark energy is deeply involved in the physics which is behind the observed structure and dynamics of clusters of galaxies. We show here that:

1. The key physical parameter of cluster of galaxies is the zero-gravity radius $R_\Lambda = \left[\frac{M}{\frac{8\pi}{3}\rho_\Lambda}\right]^{1/3}$, where M is the total matter mass of the cluster and ρ_Λ is the dark energy density which is assumed to be the same everywhere in space. A bound system must have a radius $R \leq R_\Lambda$.

2. Observational data on the Virgo cluster suggest its radius R is roughly, if not exactly, equal to system's zero-gravity radius R_Λ . For the Virgo cluster $R \simeq R_\Lambda \simeq 10$ Mpc.

3. If this is the case, the mean density of cluster's dark matter halo does not depend on the halo density profile and is determined by the dark energy density only: $\langle \rho \rangle = 2\rho_\Lambda$. The edge (cut-off) density of the

halo depends slightly on the halo profile: $\rho_{edge} = q\rho_\Lambda$, where $q = 2/3$ for the isothermal halo and around this value for the "universal" and the Einasto profiles.

4. Finally, the same considerations lead to new estimators of the local density of dark energy (40),(41), if the matter mass and the velocity dispersion (or the plasma temperature) are independently measured in a cluster. The available observational data show that the local density is near (or exactly equal to) the global value ρ_Λ . This is a new argument in favor of the interpretation of dark energy in terms of Einstein's cosmological constant.

Note, that basing on the above mentioned observational, we would not be able to distinguish between the cosmological cosmological constant, quintessence field, or phantom field, because rather narrow interval of the constant w , $P = -w\varepsilon$, obtained by observations of SN Ia and CMB fluctuations, $w = 1.08 \pm 0.12$ (Spergel et al. 2007). The quantitative data about the parameters of nearby galaxy clusters are known with a worse precision, and cannot presently be useful for this purpose. Nevertheless, a consideration of DE perturbation in the quintessence, or phantom field, see Creminelli and Senatore (2007), Creminelli et al. (2009), and their influence on the large scale structure formation, could, in principle, to be able to give a possibility to distinguish between these cases.

Acknowledgements A.C. appreciates a partial support from the RFBR grant 10-02-0178. The work of G.S.B.-K. was partially supported by RFBR grants 08-02-00491 and 11-02-00602, the RAN Program Formation and evolution of stars and galaxies and Russian Federation President Grant for Support of Leading Scientific Schools NSh-3458.2010.2.

References

- Abdalla, E., Abramo, L.R., Sodr e, L., Wang, B.: *Physics Letters B* **673**, 107 (2009)
- Antonov, V.A., Chernin, A.D.: *Soviet Astronomy Letters* **1**, 121 (1975)
- Baryshev, Y.V., Chernin, A.D., Teerikorpi, P.: *Astron. Astrophys.* **378**, 729 (2001)
- Bisnovatyi-Kogan, G.S., Zel'Dovich, Y.B.: *Astrophysics* **5**, 105 (1969)
- Byrd, G.G., Chernin, A.D., Valtonen, M.J.: *Cosmology: Foundations and Frontiers*, Moscow. U R S S (2007)
- Chernin, A., Teerikorpi, P., Baryshev, Y.: *Advances in Space Research* **31**, 459 (2003)
- Chernin, A.D.: *Physics Uspekhi* **44**, 1099 (2001)
- Chernin, A.D.: *Physics Uspekhi* **51**, 253 (2008)
- Chernin, A.D., Teerikorpi, P., Baryshev, Y.V.: *Astron. Astrophys.* **456**, 13 (2006)
- Chernin, A.D., Teerikorpi, P., Valtonen, M.J., Dolgachev, V.P., Domozhilova, L.M., Byrd, G.G.: *Astron. Astrophys.* **507**, 1271 (2009)
- Chernin, A.D., Karachentsev, I.D., Nasonova, O.G., Teerikorpi, P., Valtonen, M.J., Dolgachev, V.P., Domozhilova, L.M., Byrd, G.G.: *Astron. Astrophys.* **520**, 104 (2010)
- Creminelli, P., Senatore, L.: *J. Cosmol. Astropart. Phys.* **11**, 10 (2007)
- Creminelli, P., D'Amico, G., Noreña, J., Vernizzi, F.: *J. Cosmol. Astropart. Phys.* **2**, 18 (2009)
- Creminelli, P., D'Amico, G., Noreña, J., Senatore, L., Vernizzi, F.: *J. Cosmol. Astropart. Phys.* **3**, 27 (2010)
- Einasto, J., Haud, U.: *Astron. Astrophys.* **223**, 89 (1989)
- Ekhholm, T., Lanoix, P., Teerikorpi, P., Paturel, G., Fouqu e, P.: *Astron. Astrophys.* **351**, 827 (1999)
- Ekhholm, T., Lanoix, P., Teerikorpi, P., Fouqu e, P., Paturel, G.: *Astron. Astrophys.* **355**, 835 (2000)
- Gliner, E.B.: *Soviet Journal of Experimental and Theoretical Physics* **22**, 378 (1966)
- He, J.-H., Wang, B., Abdalla, E., Pavon, D.: *J. Cosmol. Astropart. Phys.* **12**, 22 (2010)
- Hoffman, G.L., Salpeter, E.E.: *Astrophys. J.* **263**, 485 (1982)
- Karachentsev, I.D., Nasonova, O.G.: *Mon. Not. R. Astron. Soc.* **405**, 1075 (2010)
- Karachentsev, I.D., Kashibadze, O.G., Makarov, D.I., Tully, R.B.: *Mon. Not. R. Astron. Soc.* **393**, 1265 (2009)
- Kofman, L.A., Starobinskii, A.A.: *Soviet Astronomy Letters* **11**, 271 (1985)
- Merafina, M., Bisnovatyi-Kogan, G.S., Tarasov, S.O.: *Astron. Astrophys.* **541**, 84 (2012)
- Navarro, J.F., Frenk, C.S., White, S.D.M.: *Astrophys. J.* **462**, 563 (1996)
- Perlmutter, S., Aldering, G., Goldhaber, G., Knop, R.A., Nugent, P., Castro, P.G., Deustua, S., Fabbro, S., Goobar, A., Groom, D.E., Hook, I.M., Kim, A.G., Kim, M.Y., Lee, J.C., Nunes, N.J., Pain, R., Pennypacker, C.R., Quimby, R., Lidman, C., Ellis, R.S., Irwin, M., McMahon, R.G., Ruiz-Lapuente, P., Walton, N., Schaefer, B., Boyle, B.J., Filippenko, A.V., Matheson, T., Fruchter, A.S., Panagia, N., Newberg, H.J.M., Couch, W.J., The Supernova Cosmology Project: *Astrophys. J.* **517**, 565 (1999)
- Riess, A.G., Filippenko, A.V., Challis, P., Clocchiatti, A., Diercks, A., Garnavich, P.M., Gilliland, R.L., Hogan, C.J., Jha, S., Kirshner, R.P., Leibundgut, B., Phillips, M.M., Reiss, D., Schmidt, B.P., Schommer, R.A., Smith, R.C., Spyromilio, J., Stubbs, C., Suntzeff, N.B., Tonry, J.: *Astron. J.* **116**, 1009 (1998)
- Spiegel, D.N., Bean, R., Dor e, O., Nolta, M.R., Bennett, C.L., Dunkley, J., Hinshaw, G., Jarosik, N., Komatsu, E., Page, L., Peiris, H.V., Verde, L., Halpern, M., Hill, R.S., Kogut, A., Limon, M., Meyer, S.S., Odegard, N., Tucker, G.S., Weiland, J.L., Wollack, E., Wright, E.L.: *Astrophys. J. Suppl. Ser.* **170**, 377 (2007)
- Teerikorpi, P., Chernin, A.D.: *Astron. Astrophys.* **516**, 93 (2010)
- Teerikorpi, P., Bottinelli, L., Gouguenheim, L., Paturel, G.: *Astron. Astrophys.* **260**, 17 (1992)
- Teerikorpi, P., Chernin, A.D., Karachentsev, I.D., Valtonen, M.J.: *Astron. Astrophys.* **483**, 383 (2008)
- Tully, R.B., Mohayaee, R.: In: A. Diaferio (ed.) *IAU Colloq. 195: Outskirts of Galaxy Clusters: Intense Life in the Suburbs*, p. 205 (2004)